Applied Physics Letters

Light-induced degradation and self-healing inside $CH_3NH_3PbI_3$-based solar cells

Cite as: Appl. Phys. Lett. **116**, 253303 (2020); https://doi.org/10.1063/5.0009944
Submitted: 06 April 2020 . Accepted: 14 June 2020 . Published Online: 26 June 2020

Xiaoliang Liu, Qiang Han, Yufei Liu, Chengyi Xie, Chenggang Yang, Dongmei Niu, Youzhen Li, Huanyou Wang, Lixin Xia, Yongbo Yuan, and Yongli Gao

Applied Physics Letters ARTICLE scitation.org/journal/apl

Light-induced degradation and self-healing inside $CH_3NH_3PbI_3$-based solar cells

Cite as: Appl. Phys. Lett. **116**, 253303 (2020); doi: 10.1063/5.0009944
Submitted: 6 April 2020 · Accepted: 14 June 2020 ·
Published Online: 26 June 2020

Xiaoliang Liu,[1] Qiang Han,[1] Yufei Liu,[1] Chengyi Xie,[1] Chenggang Yang,[1] Dongmei Niu,[1] Youzhen Li,[1,a)] Huanyou Wang,[2,a)] Lixin Xia,[3] Yongbo Yuan,[1] and Yongli Gao[4]

AFFILIATIONS

[1]Institute of Super-Microstructure and Ultrafast Process in Advanced Materials, School of Physics and Electronics, Central South University, Changsha 410083, People's Republic of China
[2]College of Electronic Information and Electrical Engineering, Xiangnan University, Chenzhou 423000, People's Republic of China
[3]Department of Physics, Kashgar University, Kashgar 844006, People's Republic of China
[4]Department of Physics and Astronomy, University of Rochester, Rochester, New York 14627, USA

[a)]**Authors to whom correspondence should be addressed:** liyouzhen@csu.edu.cn and whycs@163.com

ABSTRACT

$CH_3NH_3PbI_3$ ($MAPbI_3$)-based perovskite solar cells (PSCs) with special hole and electron transport layers (HTL and ETL) were prepared to study their light-induced degradation. Obvious degradation was observed under initial light exposure not only at the device level but also at the film morphology and electronic structure level. Device performance parameters, such as short-circuit current (J_{SC}), power conversion efficiency, fill factor, and hysteresis effect, were aggravated with an initial light exposure of less than ~8 h at 1 sun intensity. Meanwhile, the deteriorated crystallinity and electronic structure of the $MAPbI_3$ film were also detected with x-ray diffraction, ultraviolet photoelectron spectroscopy, and UV-Visible absorption spectroscopy. The observed degradation is rationally related to the light-induced decomposition of $MAPbI_3$. However, the degradation can be partly recovered with the following light exposure resulting in self-healing of the devices and $MAPbI_3$ films. The self-healing behavior should be ascribed to the conversion of decomposition products back to $MAPbI_3$, because the intermediates are wrapped tightly in the photoactive layer by the compact coverlayers of HTLs and ETLs and some reversible reactions occur consequently. The mechanism of self-healing is discussed by introducing the trapped states derived from ion migration. The PSCs prepared here imply a good optical stability and thus a good performance facilitated by tight wrapping of the active $MAPbI_3$.

$CH_3NH_3PbI_3$ ($MAPbI_3$)-based perovskite solar cells (PSCs) have attracted wide attention in recent years due to their decent optoelectronic properties such as a high optical absorption coefficient, long carrier diffusion lengths, and narrow bandgap.[1–8] After several years of rapid development, the power conversion efficiency (PCE) of PSCs has risen to 23.2% from 3.9% at the beginning, showing a potential to replace silicon-based solar cells.[9–12] Unfortunately, the stability of such hybrid perovskite solar cells over prolonged solar irradiation remains an urgent issue to be solved before their scalable application.[13–16] A large number of studies have found that many environmental factors, such as moisture, oxygen, temperature, and even sunlight, can lead to obvious decomposition of $MAPbI_3$ and greatly reduce the performance of PSCs.[17–20] The usual decomposition products include the ultimate formation of NH_3, CH_3I, PbI_2, and other possible degradation byproducts, often accompanied by some intermediates with different stoichiometric compositions.[21–24] Among all kinds of degradations in PSCs, the light-induced degradation deserves to be one of the most essentially unstable factors, because, after all, sunlight is a prerequisite for solar cells to operate but other factors can be largely eliminated by appropriate encapsulation technology.[25,26] Some groups reported facile photobleaching of $MAPbI_3$ in an air environment due to photo-oxidation of the iodide species.[27,28] The photochemical degradation of $MAPbI_3$ was observed by some teams even under anoxic conditions.[29–31] At the same time, many teams tried to improve the stability of PSCs by different means. Moreover, some authors reported a self-healing behavior in PSCs after some initial damage.[32,33] However, few studies have investigated the effect of light soaking on PSCs at both the device level and the film analytic level. It remains unclear to understand the mechanism of photodegradation in PSCs and to find an effective way to overcome it. Our own work on $MAPbI_3$ with surface/interfacial analysis has revealed the microscopic process of surface degradation.[34–38]

Here, we report our efforts in investigating light-induced degradation for $MAPbI_3$-based PSCs with a special hole transport layer (HTL) and an electron transport layer (ETL) at both the device level

and film analytical level. The PSCs were submitted to a short circuit to simulate their real operating conditions as being exposed to sunlight with an intensity of ~100 mW/cm^2 with different illumination durations. The characterization results showed that there were obvious photodegradation effects for both the devices and $MAPbI_3$ films with light exposure of less than ~8 h. Then, the degradation can be slowed down and partly recovered with the following light exposure, which indicates the existence of self-healing behavior in the PSCs prepared here. This self-healing behavior enhances the stability of the PSCs and improves their performance. The mechanism of self-healing was discussed further and some important insights were presented about the stability and performance of PSCs.

The $MAPbI_3$-based PSCs with a structure of indium tin oxide (ITO)/poly(bis (4-phenyl)(2,4,6-trimethylphenyl)amine)(PTAA)/$MAPbI_3$/[6,6]-phenyl-C61-butyric acid methyl ester (PCBM)/Bphen/Cu were prepared following the procedure reported previously,[39,40] where the PTAA layer and Bphen layer were used as HTL and ETL, respectively, while the PCBM layer served as the passivation layer. The $MAPbI_3$ films with a thickness of ~200 nm were fabricated using the antisolvent method with anhydrous chlorobenzene (CB) as the antisolvent.[41] Shown in the supplementary material Fig. S1(a) is the fabrication scheme of PSCs. The degradation tests were carried out following the steps as shown in Figs. S1(b)–S1(d). The as-grown PSCs were put into a glovebox with both the humidity level and oxygen level below 0.1 ppm. All the aging experiments are carried out in the glovebox. The PSCs were exposed to the illumination with an intensity of ~100 mW/cm^2 for different time durations at a short circuited state. After the characterization of photovoltaic performance, the PSCs were split to expose the active layer of $MAPbI_3$ for further characterization of the surface and interfacial properties.[42–44] The coverlayers on the $MAPbI_3$ layer were peeled off with an adhesive tape, and then the possible residues were washed away with CB.

Shown in Fig. 1 are the light exposure time-dependent photovoltaic parameters of the $MAPbI_3$-based PSCs, where the symbols denote the experimental data and the solid lines denote the fitting curves obtained by the polynomial fit. The data were achieved by averaging over the parameters of 14 samples, while each parameter was the average over forward and inverse scans. Each of the photovoltaic parameters, including the PCE, fill factor (FF), short-circuit current (J_{SC}), and open-circuit voltage (V_{oc}), indicates a distinct decrease during the initial illumination stage due to the light-induced degradation occurring in the active layer of $MAPbI_3$. The photochemical decomposition of $MAPbI_3$ inevitably leads to the damage of the structure and the migration and displacement of ions especially under the short-circuited condition; thus, there is formation of more trap states, which, in turn, deteriorates the device performance. However, the fitting curves indicate that the PCE, FF, and J_{SC} recover unexpectedly with further light exposure of more than ~8 h. The recovery of the parameter V_{oc} is also distinguishable, though it is not so obvious as the other three ones are. Therefore, we speculate rationally here that the $MAPbI_3$ films can adjust themselves to partly recover the degradation induced by light irradiation. This phenomenon has been described by the term self-healing as reported in some recent studies.[45,46]

The other evidence of self-healing occurring in $MAPbI_3$-based PSCs can be presented by the light exposure time-dependent hysteresis. It has always been known that the photocurrent hysteresis widespreadly exists in many kinds of PSCs and is rationally ascribed to the charge traps in their active layers due to the rich defects.[47,48] The hysteresis phenomenon could be identified by the difference of photocurrents between the forward and reverse scanning directions. To quantify this hysteresis behavior, here we introduce a variable as follows:

$$\delta X = |X_+ - X_-|, \quad (1)$$

where, X_+ (or X_-) denotes one of the photovoltaic parameters obtained by J–V measurements in the positive (or negative) scan.

Shown in Fig. 2 are the light exposure time-dependent δXs, i.e., (a) δJ_{sc}, (b) δV_{oc}, (c)δFF, and (d) δPCE. The evolutions of δXs have certain regularity as a whole, despite the irregularity in individual data most likely caused by some accidental factors. The process of change can be roughly divided into two stages with a turning point within the range of about 4–6 h. In the first stage, these differences increase approximately with the increase in the light exposure time, and then decrease in the following stage, which indicates that the hysteresis effect induced by light irradiation at the initial stage can be partly recovered later. It can be reasonably inferred that the defect states in PSCs have a trend of increasing first and then decreasing as PSCs are exposed to a continuous illumination, which matches with the degradation and self-healing process occurring in PSCs. This conclusion is qualitatively consistent with that obtained by the light exposure time-dependent photovoltaic parameters, although the turning point of the former is a little ahead of the latter, which means that the recovery of the hysteresis effect is slightly ahead of the photovoltaic parameters.

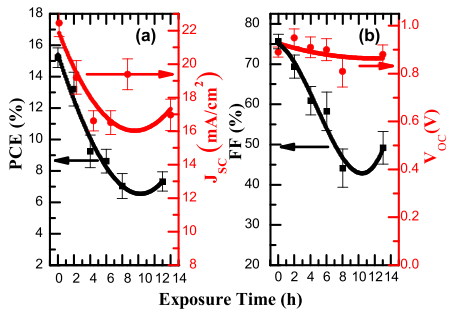

FIG. 1. Evolution of the photovoltaic parameters (a) PCE and J_{sc}, (b) FF and V_{oc} of $MAPbI_3$ based solar cells as a function of the light exposure time. The symbols denote the experimental data and the solid lines denote the fitting curves.

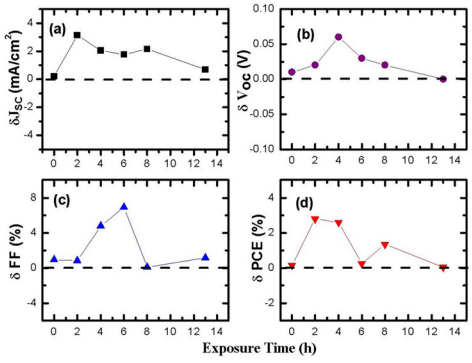

FIG. 2. Light exposure time-dependent hysteresis of the photovoltaic parameters (a) J_{sc}, (b) V_{oc}, (c) FF, and (d) PCE.

To further study the light response of $MAPbI_3$ films, the PSCs were split to expose the active layer of $MAPbI_3$ for further characterization after the light degradation test. Shown in Fig. 3 are the light exposure time-dependent XRD spectra of the $MAPbI_3$ films. The XRD pattern of the as-grown $MAPbI_3$ film confirms a dominant crystal structure of perovskite despite a low peak at a 2θ value of 12.76° [see the hash mark in Fig. 3(a)], which is assigned to the (001) crystallographic plane of PbI_2, showing a small amount of PbI_2 probably derived from the precursor PbI_2 and/or from the decomposition of $MAPbI_3$ during the annealing process. After the aging study, the XRD patterns keep similar characteristics except for some slight differences, which implies a relatively stable crystal structure of $MAPbI_3$ against light exposure. It should be noted that a new diffraction peak appears at 38.2° after a light exposure of ~4–6 h [see the asterisk marks in Fig. 3(a)], but it almost disappears with a light exposure of more than 8 h. This new diffraction peak can be assigned to the decomposition products of $MAPbI_3$ or to the mesophase structure of perovskite although its exact origin remains to be further studied. Naturally, its disappearance indicates that the degradation in $MAPbI_3$ can be partially eliminated after prolonging the illumination time.

Furthermore, a zoomed view of the (110) diffraction peak of $MAPbI_3$ is analyzed as shown in Fig. 3(b). The diffraction peak of the as-grown $MAPbI_3$ film is detected to locate at 14.08°, then the diffraction peak shifts toward the lower angle and locates at 13.92° with a light exposure of 4 h. However, it shows a shift toward the higher angle with further light exposure. The final position of the diffraction peak is detected to be 14.22° with a light exposure of 13 h. Being directly associated with the diffraction angle according to Bragg equation, the lattice parameters of $MAPbI_3$ show an increase at first but then a decrease with the following light exposure of more than ~4 h. Therefore, there is no denying the fact that the light-induced lattice changes may play a role in the device performance. We infer that some intermediate phases may appear and then disappear during a continuous illumination process, which implies the occurrence of an evolutionary process of degradation and recovery in $MAPbI_3$ films. As shown in Fig. 3(c), the intensity of the (110) diffraction peak of $MAPbI_3$ presents a similar dependence on the light exposure time with the position of the diffraction peak. The least intensity is obtained from the sample with a light exposure of ~6 h, while the intensity increases gradually with the following light exposure. This evolution also confirms that the crystallinity of the $MAPbI_3$ film deteriorates at first and then reverses with the prolonging illumination time. In addition, being similar to the conclusion for the hysteresis effect, the evolution of lattice parameters is also ahead of the photovoltaic parameters.

To study the effect of photochemical degradation on the electronic structure of the $MAPbI_3$ layer, we further collect the UPS data as shown in Fig. 4, where Figs. 4(a) and 4(b) correspond to the cutoff region and the valence band maximum (VBM) region, respectively. In order to observe the subtle change of the valence band, we enlarge the VBM region as shown in Fig. 4(c). Except for the work function (WF) of the 2-h light exposure film, the WF of the film shows a decreasing trend after light radiation of less than 6 h as shown by the dotted line arrow in Fig. 4(a). Then, it shows an increase when the light exposure time is more than 8 h until 13 h [see the solid line arrow in Fig. 4(a)]. The residues on the exposed surface of $MAPbI_3$ after the removal of coverlayers should certainly impact the WF due to its surface sensitivity. However, given the almost same test procedure in our experiments, the effect of residues on the WF should be similar for different batches of the film. So the evolution of the WF can partly reflect some physics of the $MAPbI_3$ film itself during the degradation process. We speculate that the return of the WF qualitatively describes a process of degradation and recovery. The decrease in the WF at the beginning stage can be ascribed to the degradation occurring in $MAPbI_3$ layers, and the increase in the WF at the following stage to the self-healing of $MAPbI_3$ films.

The UPS spectra obtained from the VBM region also qualitatively support the existence of a reverse process from degradation to self-healing in $MAPbI_3$ films under a continuous light exposure. The VBM of the as-grown $MAPbI_3$ film is about 1.43 eV, which is consistent with the results reported anywhere else. With a light exposure of less than 6 h, the VBM slightly shifts toward the high binding energy, which means the occurrence of n-type doping in the $MAPbI_3$ film. Some authors ascribed this kind of doping behavior to the photodegradation

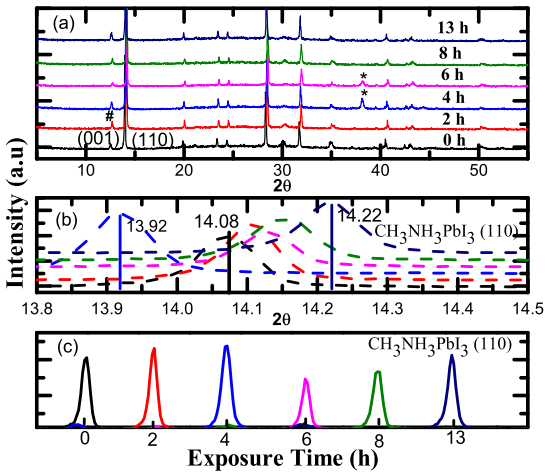

FIG. 3. Light exposure time-dependent x-ray diffraction (XRD) spectra (a), the zoomed view of the diffraction peak (110) of the $MAPbI_3$ films (b), and its intensity evolution (c).

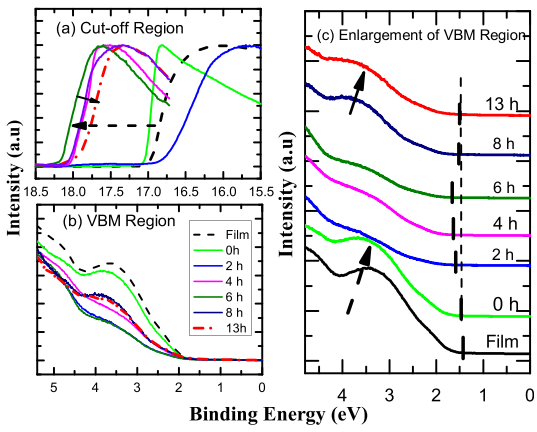

FIG. 4. Light exposure time-dependent UPS spectra of the $MAPbI_3$ film showing (a) the cutoff region, (b) the VBM region, and (c) the enlargement of the VBM region. The short lines indicate the position of VBM, and the solid line and dotted line arrows are used to attract attention.

products. For example, Wang *et al.* believed that the n-type doping might come from the lead (Pb) enrichment in the sample, similar to the case of $MAPbI_3$ annealing at a high temperature. It is worth mentioning that the VBM shifts back to a low binding energy with a further light exposure of more than 6 h. Once again, the reversal behavior of VBM rationally confirms that some photodegradation effects have be recovered. From the shape of the valence band spectrum, we can see this more intuitively. For the control film (marked as "Film" in Fig. 4) or the light exposure of 0 h, there is an obvious valence band peak at ~3.5 eV [see the dotted arrow in Fig. 4(c)]. For the 2–6 h samples, the valence band peak almost disappears, but finally, for the 8 h and 13 h ones, the valence band peak reappears [see the solid arrow in Fig. 4(c)]. The evolution of the valence band peak is closely related to the distribution of the electronic density of state in the film. Photoinduced ion migration, polarization, and other reasons might destroy the charge distribution on the surface or interface in PSCs, resulting in the change of the shape of the valence band peak. On the contrary, the self-healing behavior can partially restore the charge distribution, leading to the restoration of the valence band peak.

Moreover, as shown in Fig. S2, the evolution of absorption spectra of perovskite films with the light exposure time shows a similar reversal with the parameters of both the device and film as mentioned above. At the longer wavelength region, absorption approximately undergoes a change from increase to decrease with continuous light exposure. With an intermediate duration of light exposure, the light absorption is the strongest, which implies that the intermediate phases formed in the $MAPbI_3$ film have better absorption to long wave components of light. The evolution of optical properties observed here can most likely be ascribed to the modification of the optical bandgap of $MAPbI_3$ films during the aging tests. Using Tauc relation,[49] we obtained the optical bandgap of films, which is ~1.54 eV for the as-grown $MAPbI_3$ film, then with a small decrease after the initial light exposure, but finally with an increase following further light exposure. The decrease in the optical bandgap at the initial light exposure may be assigned with the degradation of the lattice structure and/or the emergence of the defect states between the valence band and conduction band.

Overall, it is suggested that a partial recovery of this photodegradation does occur in our aging measurements of $MAPbI_3$ based devices. To understand the mechanism of photodegradation and self-healing in PSCs, shown in Fig. 5 is the schematic of the process. Under the light radiation, $MAPbI_3$ should partly decompose into intermediates of PbI_2 and CH_3NH_3I at first,[50,51] then some volatile products of CH_3I, HI, and NH_3, and even the final products of molecular hydrogen (H_2), iodine (I_2), and metal lead (Pb) according to different reaction levels, as shown Fig. 5(a). With the photodegradation process and the ensuing defects or ion migrations, there will be some photosensitive metastable states that emerge in the $MAPbI_3$ layer, which can trap the photogenerated carriers for a relatively long time, and cause the hysteresis effect in PSCs, and eventually reduce the photovoltaic performance.[52,53]

However, in this work, the volatile products of photodegradation cannot escape easily from the active layer of $MAPbI_3$ due to its thickness of more than ~200 nm and the compact cover of the charge transport layers of PTAA and Bphen, as well as the relatively inert Cu electrode. As reported by some authors, the self-healing occurring in the $MAPbI_3$ layer is a typical bulk behavior and strongly depends on the localization of degradation products not far from the site of the damage. The special device structure and optimized fabrication process here facilitate the formation of a relatively isolated space from the unfriendly environment. Being tightly confined in the $MAPbI_3$ layer, as shown Fig. 5(b), the decomposition products should synthesize $MAPbI_3$ again with a high probability according to the reaction equation

$$NH_3(g) + CH_3I(g) + PbI_2(s) \rightarrow CH_3NH_3PbI_3(s). \quad (2)$$

Thus, the $MAPbI_3$ layer can recover to its original state to some extent as shown in Fig. 5(c). Moreover, the inert Cu electrode can effectively improve the device stability by restraining the migration of I^- ions.

The self-healing behavior of photodegradation based on the band energy diagram is shown in the bottom half of Fig. 5. With the photodegradation process, some carriers in the valence band and conduction band of the active layer of $MAPbI_3$ will be trapped in the trapped states at the first stage of photodegradation. But at the following stage of light exposure, according to the reaction shown in Eq. (2), the carriers trapped in metastable states will relax partly back to the valence band and conduction band. The accumulation under the initial illumination and dissipation away under the further illumination of the metastable trapped states is responsible for the deterioration and recovery of the perovskite solar cells, respectively. The performance of the device depends on the competition between the two opposite processes. The gradual recovery of the chemical structure and crystal structure of $MAPbI_3$ should make the photodegradation occurring in PSCs to slow down and partially recover.

In a word, we systematically studied the photodegradation effect of $MAPbI_3$-based PSCs with a structure of ITO/PTAA/$MAPbI_3$/PCBM/Bphen/Cu. After being exposed to artificial sunlight with an intensity of ~100 mW/cm^2 for different times, the devices were tested to collect their photovoltaic parameters including J–V characteristics and hysteresis. To accelerate the degradation, the PSCs are limited to work in a short circuit state as exposed to sunlight. Then, the overlayers of the PSCs are peeled off to expose the active layers of the $MAPbI_3$ layer for further characterization. It is found that the photodegradation does occur under the light exposure, but, most importantly, the initial photodegradation can be partially recovered with a prolonged light exposure. The characterization of both the $MAPbI_3$ film and the photovoltaic parameters of the $MAPbI_3$-based devices shows a self-healing behavior.

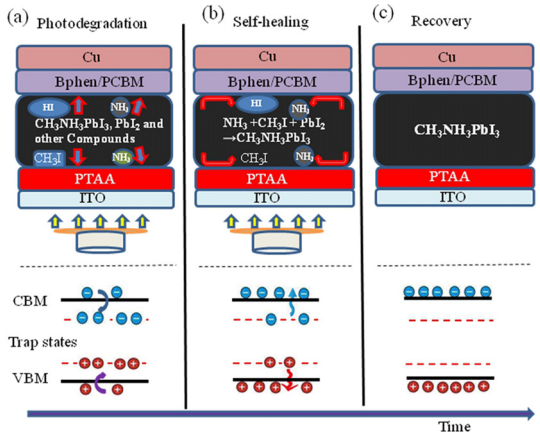

FIG. 5. Schematic of the photodegradation and self-healing in PSCs showing (a) photoinduced degradation and carrier trapping in trap states, (b) self-healing, and (c) recovery.

Owing to the special device structure along with the optimized preparation process here, the compact coverlayers on the $MAPbI_3$ layer inhibit the escape of degradation products, thus the decomposition products should synthesize $MAPbI_3$ again in the subsequent process of optical radiation. The repaired structure of $MAPbI_3$ makes the carriers trapped in the trap states relax back to the conduction band and valence band. The degradation effect produced in the early stage can be partially eliminated, so, the devices prepared by us show a relatively good photochemical stability. Of course, further explorations with a light exposure of longer time are crucial to further elaborate these issues, but our study can provide a part understanding of the degradation and recovery mechanisms in $MAPbI_3$ based solar cells.

See the supplementary material for the schematic of fabrication and degradation of the PSCs and the UV-Visible absorption spectra of $MAPbI_3$ films.

This work was supported by the National Natural Science Foundation of China (Grant No. 51673217). Y. Li acknowledges the support of the Hunan Provincial Science Foundation (Grant No. 2018JJ2505). L. Xia acknowledges the support of the National Natural Science Foundation of China (Grant No. 11564020). Y. Gao acknowledges the support of the National Science Foundation (Grant No. DMR-1903962).

DATA AVAILABILITY

The data that support the findings of this study are available from the corresponding author upon reasonable request.

REFERENCES

[1]A. Kojima, K. Teshima, Y. Shirai, and T. Miyasaka, J. Am. Chem. Soc. **131**, 6050–6051 (2009).
[2]M. Liu, M. B. Johnston, and H. J. Snaith, Nature **501**, 395 (2013).
[3]J. Burschka, N. Pellet, S.-J. Moon, R. Humphry-Baker, P. Gao, M. K. Nazeeruddin, and M. Grätzel, Nature **499**, 316 (2013).
[4]G. Hodes, Science **342**, 317–318 (2013).
[5]N. J. Jeon, J. H. Noh, W. S. Yang, Y. C. Kim, S. Ryu, J. Seo, and S. Seok, Nature **517**, 476 (2015).
[6]P. Liu, X. Liu, L. Lyu, H. Xie, H. Zhang, D. Niu, H. Huang, C. Bi, Z. Xiao, J. Huang *et al.*, Appl. Phys. Lett. **106**, 193903 (2015).
[7]J. Yan, S. Lin, X. Qiu, H. Chen, K. Li, Y. Yuan, M. Long, B. Yang, Y. Gao, and C. Zhou, Appl. Phys. Lett. **114**, 103503 (2019).
[8]Q. Wang, Y. Shao, H. Xie, L. Lyu, X. Liu, Y. Gao, and J. Huang, Appl. Phys. Lett. **105**, 163508 (2014).
[9]J. Wang, S. Luo, Y. Lin, Y. Chen, Y. Deng, Z. Li, K. Meng, G. Chen, T. Huang, S. Xiao *et al.*, Nat. Commun. **11**, 582 (2020).
[10]L. Li, C. Wang, C. Wang, S. Tong, Y. Zhao, H. Xia, J. Shi, J. Shen, H. Xie, X. Liu *et al.*, Org. Electron. **65**, 162–169 (2019).
[11]Y. Yuan, T. Li, Q. Wang, J. Xing, A. Gruverman, and J. Huang, Sci. Adv. **3**, e1602164 (2017).
[12]N. J. Jeon, H. Na, E. H. Jung, T.-Y. Yang, Y. G. Lee, G. Kim, H.-W. Shin, S. Seok, J. Lee, and J. Seo, Nat. Energy **3**, 682–689 (2018).
[13]G. Niu, X. Guo, and L. Wang, J. Mater. Chem. A **3**, 8970–8980 (2015).
[14]Y. Li, X. Xu, C. Wang, B. Ecker, J. Yang, J. Huang, and Y. Gao, J. Phys. Chem. C **121**, 3904–3910 (2017).
[15]A. Dualeh, P. Gao, S. I. Seok, M. K. Nazeeruddin, and M. Grätzel, Chem. Mater. **26**, 6160–6164 (2014).
[16]W. Tan, C. Xie, Y. Liu, Y. Zhao, L. Li, X. Liu, Y. Yuan, Y. Li, and Y. Gao, Synth. Met. **246**, 101–107 (2018).
[17]G. Niu, W. Li, F. Meng, L. Wang, H. Dong, and Y. Qiu, J. Mater. Chem. A **2**, 705–710 (2014).
[18]A. Guerrero, J. You, C. Aranda, Y. S. Kang, G. Garcia-Belmonte, H. Zhou, J. Bisquert, and Y. Yang, ACS Nano **10**, 218–224 (2016).
[19]A. M. A. Leguy, Y. Hu, M. Campoy-Quiles, M. I. Alonso, O. J. Weber, P. Azarhoosh, M. van Schilfgaarde, M. T. Weller, T. Bein, J. Nelson *et al.*, Chem. Mater. **27**, 3397–3407 (2015).
[20]B. Philippe, B.-W. Park, R. Lindblad, J. Oscarsson, S. Ahmadi, E. M. J. Johansson, and H. Rensmo, Chem. Mater. **27**, 1720–1731 (2015).
[21]M. Shirayama, M. Kato, T. Miyadera, T. Sugita, T. Fujiseki, S. Hara, H. Kadowaki, D. Murata, M. Chikamatsu, and H. Fujiwara, J. Appl. Phys. **119**, 115501 (2016).
[22]N. A. Manshor, Q. Wali, K. K. Wong, S. K. Muzakir, A. Fakharuddin, L. Schmidt-Mende, and R. Jose, Phys. Chem. Chem. Phys. **18**, 21629–21639 (2016).
[23]R. K. Misra, S. Aharon, B. Li, D. Mogilyansky, I. Visoly-Fisher, L. Etgar, and E. A. Katz, J. Phys. Chem. Lett. **6**, 326–330 (2015).
[24]S. Yang, Z. Xu, S. Xue, P. Kandlakunta, L. Cao, and J. Huang, Adv. Mater. **31**, 1805547 (2019).
[25]H. C. Weerasinghe, Y. Dkhissi, A. D. Scully, R. A. Caruso, and Y.-B. Cheng, Nano Energy **18**, 118–125 (2015).
[26]D. Yu, Y.-Q. Yang, Z. Chen, Y. Tao, and Y.-F. Liu, Opt. Commun. **362**, 43–49 (2016).
[27]C. Wang, Y. Li, X. Xu, C. Wang, F. Xie, and Y. Gao, Chem. Phys. Lett. **649**, 151–155 (2016).
[28]C. Wang and Y. Gao, J. Phys. Chem. Lett. **9**, 4657−4666 (2018).
[29]D. Bryant, N. Aristidou, S. Pont, I. Sanchez-Molina, T. Chotchunangatchaval, S. Wheeler, J. R. Durrant, and S. A. Haque, Energy Environ. Sci. **9**, 1655–1660 (2016).
[30]A. F. Akbulatov, S. Y. Luchkin, L. A. Frolova, N. N. Dremova, K. L. Gerasimov, I. S. Zhidkov, D. V. Anokhin, E. Z. Kurmaev, K. J. Stevenson, and P. A. Troshin, J. Phys. Chem. Lett. **8**, 1211–1218 (2017).
[31]A. Merdasa, M. Bag, Y. Tian, E. Källman, A. Dobrovolsky, and I. G. Scheblykin, J. Phys. Chem. C **120**, 10711–10719 (2016).
[32]D. R. Ceratti, Y. Rakita, L. Cremonesi, R. Tenne, V. Kalchenko, M. Elbaum, D. Oron, M. A. C. Potenza, G. Hodes, and D. Cahen, Adv. Mater. **30**, 1706273 (2018).
[33]S. Ghosh, Q. Shi, B. Pradhan, A. Mushtaq, S. Acharya, K. J. Karki, T. Pullerits, and S. K. Pal, J. Phys. Chem. Lett. **11**, 1239–1246 (2020).
[34]X. Liu, C. Wang, C. Wang, I. Irfan, and Y. Gao, Org. Electron. **17**, 325–333 (2015).
[35]X. Liu, C. Wang, Irfan, S. Yi, and Y. Gao, Org. Electron. **15**, 977–983 (2014).
[36]S. Wang, L. Lyu, D. Niu, L. Zhang, H. Huang, and Y. Gao, Appl. Phys. Lett. **114**, 241602 (2019).
[37]Y. Lu, Q. Han, Y. Zhao, D. Xie, J. Wei, P. Yuan, C. Yang, Y. Li, X. Liu, and Y. Gao, Results Phys. **17**, 103087 (2020).
[38]Y. Zhao, G. Feng, and J. Jiang, Solid State Electron. **165**, 107767 (2020).
[39]Y. Shao, Y. Yuan, and J. Huang, Nat. Energy **1**, 15001 (2016).
[40]C. Xie, C. Zhou, B. Yang, L. Shen, L. Ke, L. Ding, and Y. Yuan, Appl. Phys. Express **12**, 064006 (2019).
[41]M. Xiao, F. Huang, W. Huang, Y. Dkhissi, Y. Zhu, J. Etheridge, A. Gray-Weale, U. Bach, Y. B. Cheng, and L. Spiccia, Angew. Chem. **53**, 9898–9903 (2014).
[42]Y. Zhao, X. Liu, L. Lyu, L. Li, W. Tan, S. Wang, C. Wang, D. Niu, H. Xie, H. Huang *et al.*, Synth. Met. **229**, 1–6 (2017).
[43]Y. Liu, H. Zai, H. Xie, B. Liu, S. Wang, Y. Zhao, D. Niu, H. Huang, Q. Chen, and Y. Gao, Org. Electron. **73**, 327–331 (2019).
[44]X. Liu, S. Yi, C. Wang, C. Wang, and Y. Gao, J. Appl. Phys. **115**, 163708 (2014).
[45]W. Nie, J.-C. Blancon, A. J. Neukirch, K. Appavoo, H. Tsai, M. Chhowalla, M. A. Alam, M. Y. Sfeir, C. Katan, and J. Even, Nat. Commun. **7**, 11574 (2016).
[46]Y. Liu, C. Xie, W. Tan, X. Liu, Y. Yuan, Q. Xie, Y. Li, and Y. Gao, Org. Electron. **71**, 123–130 (2019).
[47]Y. Shao, Z. Xiao, C. Bi, Y. Yuan, and J. Huang, Nat. Commun. **5**, 5784 (2014).
[48]X. Zheng, B. Chen, J. Dai, Y. Fang, Y. Bai, Y. Lin, H. Wei, X. Zeng, and J. Huang, Nat. Energy **2**, 17102 (2017).
[49]J. Tauc, "Optical properties of amorphous semiconductors," *Amorphous Liquid Semiconductor* (Springer, USA, 1974), pp. 159–220.
[50]W. Xu, L. Liu, L. Yang, P. Shen, B. Sun, and J. A. McLeod, Nano Lett. **16**, 4720−4725 (2016).
[51]E. J. Juarez-Perez, Z. Hawash, S. R. Raga, L. K. Ono, and Y. Qi, Energy Environ. Sci. **9**, 3406–3410 (2016).
[52]Y. Yuan and J. Huang, Acc. Chem. Res. **49**, 286–293 (2016).
[53]K. Domanski, B. Roose, T. Matsui, M. Saliba, S.-H. Turren-Cruz, J.-P. Correa-Baena, C. R. Carmona, G. Richardson, J. M. Foster, and F. De Angelis, Energy Environ. Sci. **10**, 604 (2017).